



Cite this: *Org. Biomol. Chem.*, 2016,  
14, 7563

## Complexation of clofazimine by macrocyclic cucurbit[7]uril reduced its cardiotoxicity without affecting the antimycobacterial efficacy†

Shengke Li,<sup>a</sup> Judy Yuet-Wa Chan,<sup>a</sup> Yan Li,<sup>b</sup> David Bardelang,<sup>c</sup> Jun Zheng,<sup>b</sup> Wing Wai Yew,<sup>d</sup> Denise Pui-Chung Chan,<sup>d</sup> Simon Ming Yuen Lee<sup>a</sup> and Ruibing Wang<sup>\*a</sup>

Cucurbit[7]uril (CB[7]) has recently attracted increasing attention in pharmaceutical sciences due to its great potential in improving the physicochemical properties and bioactivity of drug molecules. Herein, we have investigated the influence of CB[7]'s complexation on the solubility, antimycobacterial activity, and cardiotoxicity of a model anti-tuberculosis drug, clofazimine (CFZ), that has poor water-solubility and inherent cardiotoxicity. In our study, CFZ was found to be complexed by CB[7], in a 1:1 binding mode with a relatively strong binding affinity (in the order of magnitude of  $10^4$ – $10^5$  M<sup>-1</sup>), as determined by the phase solubility method via HPLC-UV analysis and <sup>1</sup>H NMR titration, as well as UV-visible spectroscopic titration, and further confirmed by electrospray ionization mass spectrometry (ESI-MS). Upon complexation, the solubility of virtually insoluble CFZ was significantly increased, reaching a concentration of up to approximately 0.53-fold of the maximum solubility of CB[7]. The inherent cardiotoxicity of CFZ was dramatically reduced to almost nil in the presence of CB[7]. Importantly, on the other hand, such a supramolecular complexation of the drug did not compromise its therapeutic efficacy, as shown by the antimycobacterial activities examined against *Mycobacterium smegmatis*, demonstrating the significant potential of CB[7] as a functional pharmaceutical excipient.

Received 15th May 2016,

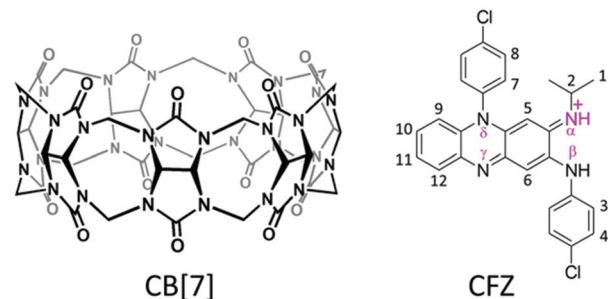
Accepted 14th July 2016

DOI: 10.1039/c6ob01060a

[www.rsc.org/obc](http://www.rsc.org/obc)

## Introduction

Clofazimine (CFZ), a riminophenazine agent (Scheme 1), which was initially developed for the treatment of tuberculosis (TB),<sup>1–3</sup> has been recommended for decades by the World Health Organization for the therapy of multibacillary leprosy.<sup>4</sup> Recent studies have revived its application in the treatment of multidrug-resistant TB, where it shows very high effectiveness along with significantly short therapeutic duration.<sup>5,6</sup> However, due to its extremely poor aqueous solubility and high lipophilicity ( $\log P > 7$ ), CFZ is classified as a class II drug (Bio-



**Scheme 1** Molecular structures of cucurbit[7]uril (CB[7]) and the most stable isomer of mono-protonated CFZ with hydrogen and nitrogen atoms numerically and symbolically labeled respectively.<sup>10,16</sup>

<sup>a</sup>State Key Laboratory of Quality Research in Chinese Medicine, Institute of Chinese Medical Sciences, University of Macau, Taipa, Macau SAR, China.

E-mail: [rwang@umac.mo](mailto:rwang@umac.mo)

<sup>b</sup>Faculty of Health Sciences, University of Macau, Taipa, Macau SAR, China

<sup>c</sup>Aix-Marseille Université, CNRS, Institut de Chimie Radicalaire, UMR 7273, 13013 Marseille, France

<sup>d</sup>Stanley Ho Centre for Emerging Infectious Diseases, The Chinese University of Hong Kong, Hong Kong, China

† Electronic supplementary information (ESI) available: Phase solubility diagram by the NMR method, representative <sup>1</sup>H NMR and HPLC-UV spectra, UV-visible titration data, the details of DFT calculations for the most stable conformer of the singly charged clofazimine, and the two most likely inclusion complexes (CFZ + H)<sup>+</sup> @CB[7]. See DOI: 10.1039/c6ob01060a

pharmaceutics Classification System) with low bioavailability and a slow rate of elimination.<sup>7</sup> Clinical studies have revealed that long-term administration and associated high-concentration bioaccumulation of CFZ resulted in yellowish and reddish skin pigmentation (require >2 years for elimination), abdominal pain and cardiotoxicity.<sup>2,8–13</sup> To circumvent the poor bioavailability as well as the side-effects of CFZ, a plethora of strategies, including molecular structure modification,<sup>14,15</sup> salt preparation,<sup>16</sup> nanosuspension,<sup>17</sup> and solid



dispersion,<sup>18–21</sup> have been attempted to improve the solubility and minimize the side-effects of CFZ. Additionally, encapsulation by drug delivery vehicles such as amphiphilic polymers,<sup>22–26</sup> liposomes,<sup>27,28</sup> and macrocyclic molecules<sup>29,30</sup> has also been considered as a promising solution for bioavailability improvement, and to confer probable benefits on the management of side effects. Among these novel drug delivery vehicles, macrocyclic molecules have recently stimulated great interest in the pharmaceutical research field, as complexation by such molecules may not only improve the physicochemical properties of an active pharmaceutical ingredient (API), but also may modulate the biological activities of encapsulated APIs.<sup>31</sup> For instance, the solubility of CFZ is significantly enhanced upon its complexation with the parent and modified cyclodextrins (CDs).<sup>29,32</sup> However, clinical benefits on the drug's efficacy and side effect management haven't been demonstrated with this strategy.

As a novel family of macrocycles, cucurbit[n]uril (CB[n],  $n = 5\text{--}8, 10, 14$ ), emerged as a competitive candidate for the next generation of medical excipients in the pharmaceutical research field.<sup>31,33–37</sup> CB[n] consist of  $n$  glycoluril units connected by  $2n$  methylene groups *via* nitrogen atoms, forming a pumpkin shaped macrocycle with one hydrophobic cavity accessible through two identical portals each fringed by  $n$  carbonyl groups. CB[7] (Scheme 1), with superior aqueous solubility and proven biocompatibility amongst the CB[n] family members,<sup>38–40</sup> may include a wide range of *N*-containing APIs with relatively higher binding affinities than those with CDs.<sup>34,41</sup> Accordingly, CB[7]'s ability to modulate or improve the physicochemical properties of complexed APIs has been extensively investigated by numerous researchers.<sup>41</sup> For instance, we have discovered the  $pK_a$  shift of ranitidine,  $\beta$ -carboline, benzocaine and its metabolite *para*-aminobenzoic acid, and a thiazolium based model drug, upon their supramolecular complexations with CB[7],<sup>42–46</sup> as well as supramolecular encapsulation driven base-on/off conversion of vitamin B<sub>12</sub> and coenzyme B<sub>12</sub>.<sup>47–49</sup> However, *in vitro* and *in vivo* studies to directly demonstrate the potential biomedical benefits of such supramolecular encapsulations by CB[n] have been relatively rare, since Kim and Day research groups pioneered studies of *in vitro* evaluation of platinum-based anti-cancer drugs with/without CB[n].<sup>50,51</sup> Recently CB[n] and its analogues have been investigated for their potential as reversal agents to neuromuscular blocking agent (NMBA),<sup>52,53</sup> and inhibitory agents of amyloid fibrillation.<sup>54</sup> By virtue of zebra fish models, our group has recently reported the use of CB[7] for reversal of general anesthesia *in vivo*,<sup>55</sup> inhibition of neurodegeneration induced by MPTP/MPP<sup>+</sup> *in vivo*,<sup>56</sup> and for enhanced uptake of a natural model drug coumarin-6 both *in vitro* and *in vivo*.<sup>57</sup> In this study, we further extended our research efforts into investigation of the influence of supramolecular complexation of CFZ by CB[7] on the water solubility, antimycobacterial activity and cardiotoxicity of the riminophenazine congener, *in vitro* and *in vivo*, respectively. This study may provide a facile solution for toxicity reduction of CFZ, while maintaining its antimycobacterial activity, thus alluding to the potential of CB[n]s.

and other macrocyclic molecules as functional pharmaceutical excipients.

## Experimental

### Materials and methods

A literature method was employed for preparing the host molecule CB[7].<sup>58</sup> Commercially available clofazimine (CFZ) was used as received. A Bruker 600 MHz NMR spectrometer was used to record the 1D <sup>1</sup>H NMR and 2D COSY/HSQC/HMBC/NOESY/ROESY spectra. Meanwhile, a Thermo LTQ Orbitrap XL equipped with an ESI/APCI multiprobe was used to acquire ESI-MS spectra. HPLC experiments were performed with an Agilent 1200 series HPLC (Agilent Technologies, Santa Clara, California), and the integration of the peaks was processed with the built-in software. The modelled structures of the complexes demonstrated in this investigation were calculated by energy-minimizations using DFT (B3LYP/6-31G(d)) level of theory within the Gaussian09 Rev.D01 package program, which were conducted at the computing facility of Aix-Marseille Université, France.

### Phase solubility experiments

**HPLC method.** A standard curve of CFZ was established at first with a HPLC-UV method. Subsequently, a 2 mM stock solution of CB[7] in an acid solution (pH = 2.0) was prepared. Various concentrations of CB[7] (2.0, 1.6, 1.0, 0.8, 0.5, and 0.2 mM) that was diluted from the stock solution were employed to dissolve excess amounts of CFZ in respective vials. The solutions were sonicated for 3 min and shaken overnight until equilibrium was reached. The solutions were centrifuged (13 200 rpm, 10 min), 0.3 ml supernatant was aliquoted from each solution, and was added to 0.2 ml (6.0 mM, pH = 2) 1-adamantylamine solution. The mixtures were vortexed for 1 min and sonicated for 3 min. 0.3 ml CH<sub>3</sub>CN was added to the mixture to dissolve all the precipitated CFZ, and the resulting solution was filtered for HPLC experiment. The CFZ was separated on a ZORBAX Eclipse XDB-C18 column (150 × 4.6 mm, 5  $\mu\text{m}$ ; Agilent Technologies) with a mobile phase at pH = 3 (formic acid was added) (A) and acetonitrile (B). A gradient method was used with a flow rate of 0.8 mL min<sup>−1</sup>. Initially, composition of solvent B was increased from 20% to 80% for 4 min, maintained for 3 min, then decreased to 20% in 1 min and maintained for 4 min. The temperatures of the column and auto-sampler were maintained at room temperature (see Fig. S1† for a representative chromatogram).

**NMR method.** In order to prepare solutions for constructing a phase solubility diagram with the help of a <sup>1</sup>H NMR test, a 4 mM solution of CB[7] with 3.7 mM sodium acetate in a D<sub>2</sub>O/DCl solution (pD = 2.0) was prepared. Various concentrations of CB[7] (1.0, 1.5, 2.0, 2.5, 3, and 4 mM) that was diluted from the stock solution were employed to dissolve excess amounts of CFZ (>6 mM) in respective vials. The solutions were shaken overnight until equilibrium was reached.



The solutions were centrifuged, and the supernatant was used for the  $^1\text{H}$  NMR test. The concentration of CFZ and CB[7] in the supernatant could be calculated *via* the ratio between the integration of CFZ protons and that of internal standard sodium acetate with a known concentration (see Fig. S2† for a representative spectrum).

### ESI-MS experiments

CB[7] (1 mM) in formic acid solution, was employed to dissolve the excess amount of CFZ. The resulting solution was filtered, and 10-fold diluted for ESI-MS determination. ESI-MS analytical parameters: ionization spray voltage 4.5 kV, capillary temperature 275 °C, and sheath gas pressure ( $\text{N}_2$ ) 5 arb.

### Strains and growth conditions

*Mycobacterium smegmatis* MC<sup>2</sup>155 was used for the bacterial drug susceptibility test. *M. smegmatis* was cultured at 37 °C in Middlebrook 7H9 broth supplied with 0.2% glycerol, 0.05% Tween 80, and 10% ADS (albumin–dextrose–saline).

### Drug susceptibility test

Bacterial drug susceptibility against CFZ in the absence and presence of CB[7] was determined in 7H9 medium as described previously.<sup>59</sup> Briefly, CFZ and CFZ@CB[7] dissolved in DMSO were 2-fold serially diluted and spotted in 96-well plates, resulting in 10 dilutions of each of the compounds. A volume of 200  $\mu\text{l}$  of *Mycobacterium smegmatis* MC<sup>2</sup>155 culture at final  $\text{OD}_{600} = 0.02$  was added to each well containing the testing compounds. The plates were then incubated at 37 °C for 48 h and the growth of bacteria ( $\text{OD}_{600}$  value) was recorded using a Tecan Infinite M200 PRO Multifunctional Microplate Reader. The minimum inhibition concentration ( $\text{MIC}_{50}$ ) curves were plotted using GraphPad Prism 5 software.

### Zebrafish maintenance and husbandry

Zebrafish facilities at the Institute of Chinese Medical Sciences (ICMS) were maintained as described in the Zebrafish Handbook. All zebrafish embryos were collected after natural spawning, staged according to the standard criteria, and raised synchronously at 28.5 °C in embryo medium. A transgenic line Tg (*cmlc2*:GFP), in which green fluorescent protein (GFP) expresses in the myocardium, was used for cardiac functional tests. All experiments involving animals were conducted according to the ethical guidelines of the Institute of Chinese Medical Sciences, University of Macau.

### Measurement of cardiac toxicity

Tg (*cmlc2*:GFP) zebrafish larvae were used for the cardiotoxicity assay. Zebrafish embryos were cultivated in embryo medium containing 0.003% (wt%) of 1-phenyl-2-thiourea (PTU) to block pigmentation since 1 dpf. Meanwhile, 2 dpf zebrafish larvae were dechorionated as mentioned above, and then randomly distributed into a 24-well microplate (12 to 14 fish per well), treated with various concentrations of CFZ in the presence or absence of CB[7]. After 2 days of incubation, zebrafish were immersed into a 1% (wt%) low-melting point agarose matrix

(Gibco) to fix them in a dorsal orientation and restrict their movement. The heart morphology, heart rates (HR) and quantitative assessment of other cardiac functions were obtained from 15 s video segments recorded of individual fish using an Olympus Cell<sup>®</sup>R imaging system comprising an IX71 microscope at room temperature. Ventricular functions were evaluated with various parameters, which were measured as described below. Images from the video were used to measure the longitudinal axis length (a) and lateral axis length (b) between the myocardial borders of ventricles at end-diastole and end-systole, respectively. In order to measure the HR, the number of heartbeats in a 15 s interval was counted. The ventricular volume at end-diastole (EDV) and end-systole (ESV) in the larvae was calculated from the heart dimensions using the formula for a prolate spheroid:  $V = 4/3\pi ab^2$ . The stroke volume (SV), cardiac output (CO) and percent fractional shortening (%FS) were calculated as follows:  $SV = (EDV - ESV)$ ,  $CO = SV \times HR$ ,  $%FS = (\text{Diastolic diameter} - \text{Systolic diameter})/(\text{Systolic diameter}) \times 100\%$ .

## Results and discussion

### $^1\text{H}$ NMR titration of the host–guest complex

Before the  $^1\text{H}$  NMR titration was conducted, CFZ was dissolved in aqueous solutions (neutral and acidic) in the absence and presence of CB[7]. As shown in Fig. 1, under acidic conditions, CFZ became moderately soluble as evidenced by the light purple color of the solution, in comparison with the apparently insoluble appearance under neutral conditions. The improved solubility of CFZ was likely due to amine protonation under acidic conditions.<sup>10,25,60</sup> In the presence of CB[7] under both neutral and acidic conditions, the color of the solutions deepened significantly, which was mainly attributed to the dissolution of CFZ when complexed with CB[7] (Fig. 1).<sup>25</sup>

Given that CFZ is virtually insoluble in aqueous solution,  $^1\text{H}$  NMR titration of CFZ was performed at  $pD = 2$  with increasing amount of CB[7] in  $\text{D}_2\text{O}$ . However, the obtained  $^1\text{H}$  NMR spectrum of CFZ alone (Fig. 2a) suggested that CFZ's solubility, even under acidic conditions, was rather poor and the dissolved CFZ quantity was still well under the detection limit of

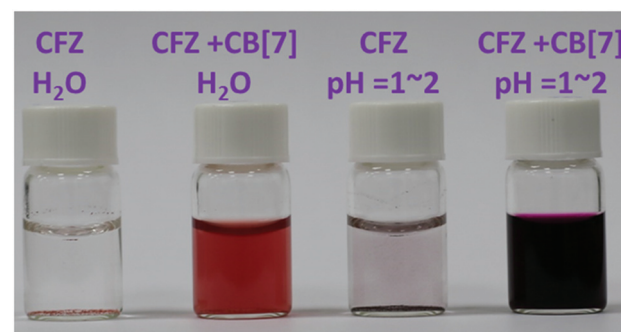
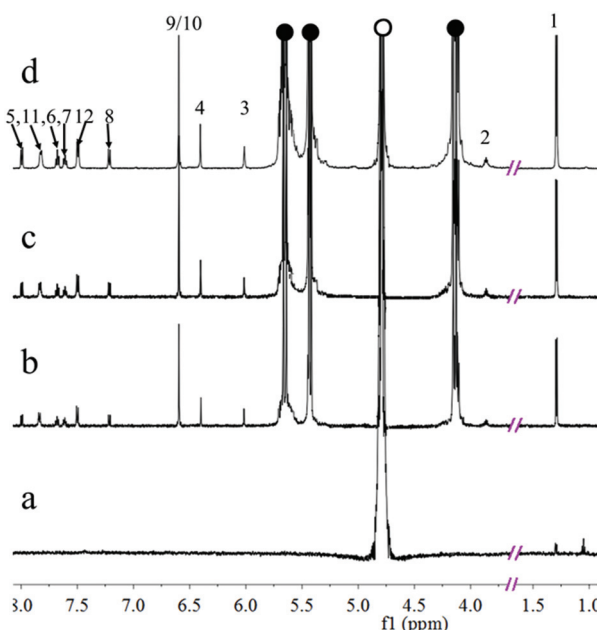


Fig. 1 Dissolution of CFZ (2 mM) in aqueous solutions (neutral and acidic) in the absence and in the presence of CB[7] (4 mM).





**Fig. 2**  $^1\text{H}$  NMR spectra of CFZ in the absence (a) and in the presence of 0.5 equiv. (b), 1.2 equiv. (c) and 2.2 equiv. (d) of CB[7] ( $\text{pD} = 2$ ). Resonances of CB[7] and HOD protons are labelled as (●) and (○), respectively. The CFZ proton resonances are assigned according to COSY/HSQC/HMBC NMR.

NMR spectroscopy (600 MHz), although the number of scans was increased to 512. Upon gradual addition of CB[7] (up to 2.2 equivalents, Fig. 2b-d), the proton resonances of the host-guest complexes became detectable, accompanied by increased resonance intensities without chemical shift changes, in line with dramatic improvements of CFZ's aqueous solubility. The unchanged chemical shift of all guest protons upon addition of >2.2 equivalents CB[7] may suggest a 1:1 binding stoichiometry between CB[7] and CFZ. Additionally, 2D NOESY and ROESY NMR experiments failed to identify NOE interactions between any of the protons of CB[7] and the guest protons presumably due to weak cross-peaks, similar to what we have observed previously in the CB[7]-bis(thiazolium) salt complexation system,<sup>46</sup> although such NOE was identified before in some other CB[7]-based host-guest complexes.<sup>61,62</sup> We therefore attempted to use Density Functional Theory (DFT B3LYP/6-31G(d)) to calculate the most probable complexation geometry between CFZ and CB[7], and the results suggested that the Cl-Phe-NH ( $\beta$ ) portion of CFZ is likely encapsulated by the cavity of CB[7] (Fig. S3,<sup>†</sup> and calculation and associated discussion details are provided in the ESI<sup>†</sup>).

### Binding parameters determination

Endeavors to gain further insights by isothermal titration calorimetry were unsuccessful due to the poor solubility of CFZ. However, as discussed in the previous section, visual inspections and  $^1\text{H}$  NMR spectra showed that CB[7] enhanced the solubility of CFZ upon forming host-guest complexes. Therefore, phase solubility diagrams were constructed to deter-

mine the binding stoichiometry and the binding strength.<sup>63</sup> In a phase solubility diagram, the solubility of a guest exhibiting a linear increase upon gradual addition of a host would suggest a 1:1 binding mode between the host and the guest molecules. The binding affinity  $K_a$  may be calculated according to the slope of such a phase diagram and the intrinsic solubility of the guest by eqn (1).<sup>64</sup> Generally, for both HPLC and NMR methods, an increasing quantity of CB[7] was added to a large excess of insoluble CFZ in acidic solution (in  $\text{H}_2\text{O}$  or  $\text{D}_2\text{O}$ ), and the mixture was shaken at room temperature until it reached equilibrium. After centrifugation, the concentration of CFZ in the supernatant was determined by both HPLC and NMR methods.

$$K_a = \frac{\text{Slope}}{S_0(1 - \text{Slope})} \quad (1)$$

As shown in Fig. 3 and Fig. S4,<sup>†</sup> the plots of the CFZ concentration against that of CB[7] show a linear trend for both HPLC and NMR experiments, indicating a 1:1 binding stoichiometry, which is consistent with the NMR data (Fig. 2).

It was reported that the solubility of protonated CFZ under acidic conditions is 20 mg  $\text{L}^{-1}$ .<sup>25</sup> The phase solubility data based on the HPLC-UV method and  $^1\text{H}$  NMR titration method afforded the binding constant  $K_a$  of  $2.66 (\pm 0.13) \times 10^4 \text{ M}^{-1}$  and  $3.15 (\pm 0.16) \times 10^5 \text{ M}^{-1}$ , respectively. HPLC analysis is often considered as a more accurate quantification method in comparison with other means, thus we believe that the binding constant is likely in the order of magnitude of  $10^4 \text{ M}^{-1}$ . Additionally, we managed to develop UV-visible titration of CFZ by CB[7] in 5 M HCl solution (Fig. S5<sup>†</sup>). The plot of the absorbance of CFZ at 530 nm against the CB[7] concentration supported 1:1 binding stoichiometry and yielded a binding constant  $K_a$  of  $5.40 (\pm 0.20) \times 10^4 \text{ M}^{-1}$ , which is in the same magnitude order with the  $K_a$  determined by the HPLC-UV phase solubility method.

Electrospray Ionization-Mass Spectrometry (ESI-MS) analysis was also used to get further insights into the binding stoichiometry. As shown in Fig. 4, a doublet charged peak was found at  $m/z = 818.24$ , corresponding to the  $\{\text{CFZ}@\text{CB}[7]\}^+$

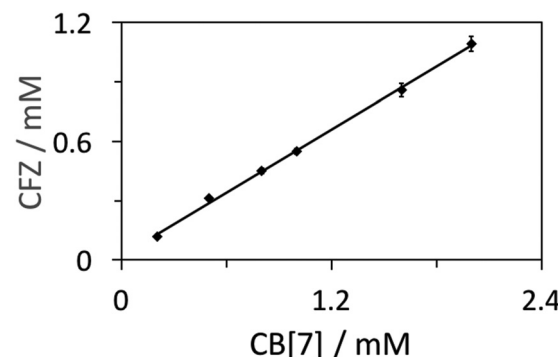


**Fig. 3** Phase-solubility diagrams of CFZ and CB[7], determined from HPLC-UV chromatogram integrations (the linear fit equation:  $y = 0.5294x + 0.026$ ,  $R^2 = 0.9985$ ).



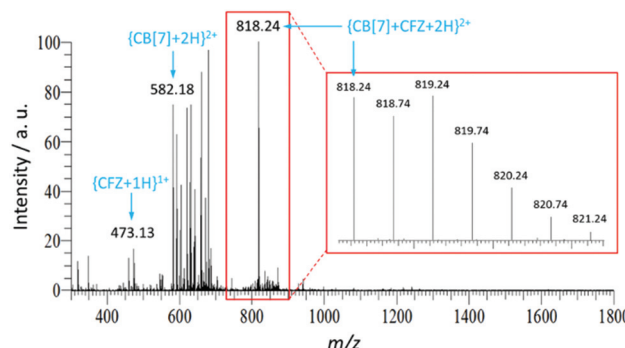


**Fig. 4** ESI-MS spectrum of a mixture of CB[7] and CFZ. Formic acid was added for the protonation of CFZ. The singlet charged peak at  $m/z = 473.13$  is likely due to  $\{\text{CFZ} + 1\text{H}\}^{1+}$  (calculated  $m/z = 473.13$ ), and the doublet charged peak at  $m/z = 582.18$  assigned to  $\{\text{CB}[7] + 2\text{H}\}^{2+}$  (calculated  $m/z = 582.18$ ).

$2\text{H}_\text{J}^{2+}$  complex (calculated  $m/z = 818.24$ ) in line with a 1:1 binding mode.

### Effect of CB[7] on cardiac toxicity of CFZ *in vivo*

To evaluate the effect of supramolecular complexation of CFZ by CB[7] on its inherent cardiotoxicity, a transgenic zebrafish model was adopted as a facile *in vivo* model for cardiac function examinations of zebrafish treated with CFZ in the absence and in the presence of CB[7]. Zebrafish has become a widely used animal model for drug discovery and efficacy/toxicity evaluations because of its physiological and genetic similarity to mammals, cost-effectiveness and ease of handling.<sup>65</sup> Changes in physiological functions, phenotypes and genetic expression are highly useful indicators for toxicity.<sup>66,67</sup> Heart rate, stroke volume, cardiac output and fractional shortening are often monitored as a set of physiological parameters to evaluate cardiac toxicities.<sup>68</sup>

By analyzing the videos and images of the fish hearts recorded, the cardiac functions were evaluated. Fig. 5 shows that CFZ induced cardiac malfunctions in a dose-dependent manner, as was evaluated from the heart rate (5a), stroke volume (5b), cardiac output (5c) and fractional shortening (5d), with toxic effects most pronounced at a 16.90  $\mu\text{M}$  level showing significantly reduced stroke volume, cardiac output and fractional shortening as well as a moderate heart rate decrease. Thus, at this toxic concentration level, the influence of CB[7] on CFZ's cardiotoxicity was evaluated. When the zebrafish larvae were incubated with CFZ (16.90  $\mu\text{M}$ ) in the presence of 100  $\mu\text{M}$  CB[7], the cardiac functions were significantly improved when compared to CFZ alone ( $p < 0.05$ ), and nearly restored back to the normal state (similar to those of the control group). Additionally, it is worth noting that the cardiac functions of zebrafish larvae treated with 100  $\mu\text{M}$  CB[7] alone were similar to those of the blank control group, implying that CB[7] at this concentration has a negligible effect on cardiac functions of zebrafish.

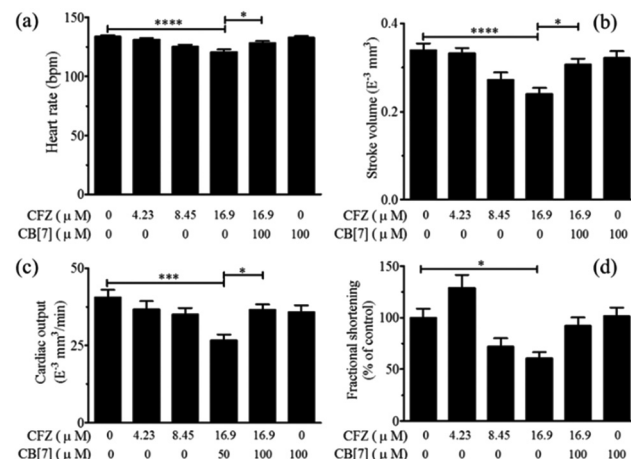


**Fig. 5** Cardiac functions of zebrafish larvae exposed to various concentrations of CFZ, and CB[7]. Heart rate (a), stroke volume (b), cardiac output (c) and % fractional shortening (d) were calculated from the video and images of the zebrafish heart recorded. Data are expressed as mean  $\pm$  S.E.M. ( $n = 10-15$ ). \* $p < 0.05$ , \*\* $p < 0.01$ , \*\*\* $p < 0.001$ , \*\*\*\* $p < 0.0001$ .

### Effect of CB[7] on the antimycobacterial activity of CFZ *in vitro*

To examine the influence of supramolecular complexation of CFZ by CB[7] on its antimycobacterial activity, the minimal inhibitory concentrations of CFZ against 50% of bacillary strains ( $\text{MIC}_{50}$ ) in the absence and in the presence of CB[7] were examined against *Mycobacterium smegmatis*, a non-pathogenic mycobacterial strain that biologically resembles *Mycobacterium tuberculosis*. CB[7] alone was used for comparison and the result showed that it didn't have any antimycobacterial activity (Fig. 6). In the presence of CB[7], CFZ demonstrated a  $\text{MIC}_{50}$  of  $1.31 \times 10^{-6}$  M, moderately lower but comparable to that of free CFZ ( $\text{MIC}_{50}$  of  $2.09 \times 10^{-6}$  M, Fig. 6). A statistical analysis of their  $\text{MIC}_{50}$  values from triplicates did not show significant difference between the two groups, suggesting that

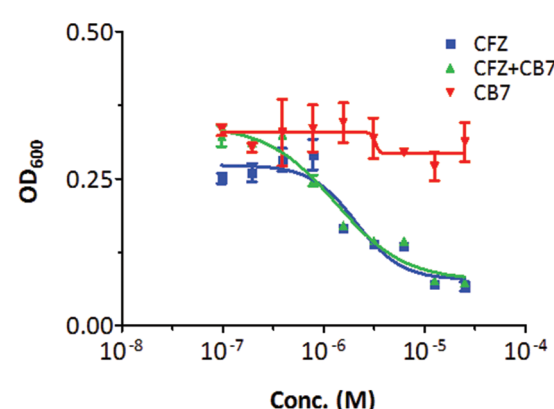


**Fig. 6** Effect of CB[7] on the antimycobacterial activity of CFZ, examined on *M. smegmatis* (cultured at 37 °C in Middlebrook 7H9 broth supplied with 0.2% glycerol, 0.05% Tween 80, and 10% ADS (albumin-dextrose-saline)).



CB[7] complexation had little effect on the antimycobacterial activities of CFZ, which is similar to what was observed with cyclodextrin complexed CFZ.<sup>29</sup>

## Conclusions

In summary, we reported that clofazimine (CFZ) forms 1:1 complexes with cucurbit[7]uril (CB[7]), with the binding affinity in the magnitude orders of  $10^4$ – $10^5$  M<sup>-1</sup> under acidic conditions. More significantly, the inherent cardiac toxicity of CFZ was dramatically alleviated upon its complexation with CB[7] when evaluated with an *in vivo* transgenic zebrafish model, whereas its therapeutic efficacy was well preserved, as examined against *Mycobacterium tuberculosis* and *Mycobacterium smegmatis* *in vitro*. Our study provides a facile solution for improving physicochemical properties of CFZ, such as water-solubility, and for alleviation of its inherent side effects while maintaining its efficacy. This discovery may further promote research efforts for exploring CB[n]s and other novel macrocyclic molecules as the next-generation functional pharmaceutical excipients.

## Conflict of interest

The authors declare no competing financial interest.

## Acknowledgements

The authors are grateful for the financial support received from the University of Macau Research Fund (project No. SRG2014-00025-QRCM-ICMS), and Macau Science and Technology Development Fund (FDCT/020/2015/A1 and FDCT 066/2015/A2), as well as the SKL-QRCM Open Fund (SKL Open-003).

## Notes and references

- V. C. Barry, J. G. Belton, M. L. Conalty, J. M. Denneny, D. W. Edward, J. F. O'Sullivan, D. Twomey and F. Winder, *Nature*, 1957, **179**, 1013–1015.
- R. O'Connor, J. F. O'Sullivan and R. O'Kennedy, *Drug Metab. Rev.*, 1995, **27**, 591–614.
- D. Kumar, B. Negi and D. S. Rawat, *Future Med. Chem.*, 2015, **7**, 1981–2003.
- WHO, *Model Prescribing Information: Drugs Used in Leprosy*, World Health Organization, 1998.
- T. Dey, G. Brigden, H. Cox, Z. Shubber, G. Cooke and N. Ford, *J. Antimicrob. Chemother.*, 2013, **68**, 284–293.
- S. Tyagi, N. C. Ammerman, S. Y. Li, J. Adamson, P. J. Converse, R. V. Swanson, D. V. Almeida and J. H. Grosset, *Proc. Natl. Acad. Sci. U. S. A.*, 2015, **112**, 869–874.

- Clofazimine, Biopharmaceutics Classification System database, <http://www.ddfint.org/bcs-database/>.
- K. A. Min, W. G. Rajeswaran, R. Oldenbourg, G. Harris, R. K. Keswani, M. Chiang, P. Rzeczycki, A. Talatoff, M. Hafeez, R. W. Horobin, S. D. Larsen, K. A. Stringer and G. R. Rosania, *Adv. Sci.*, 2015, **2**, 1500025.
- G. Ramachandran and S. Swaminathan, *Drug Saf.*, 2015, **38**, 253–269.
- R. K. Keswani, J. Baik, L. Yeomans, C. Hitzman, A. M. Johnson, A. S. Pawate, P. J. Kenis, N. Rodriguez-Hornedo, K. A. Stringer and G. R. Rosania, *Mol. Pharm.*, 2015, **12**, 2528–2536.
- J. Y. W. Chan, R. K. K. Leung, J. Li, A. W. H. Chan, S. S. Lee, R. Wang, S. M. Y. Lee, D. P. C. Chan and W. W. Yew, *J. Antimicrob. Chemother.*, 2016, submitted.
- R. S. Wallis, *Clin. Infect. Dis.*, 2013, **56**, 106–113.
- S. H. Choudhri, L. Harris, J. W. Butany and J. S. Keystone, *Lepr. Rev.*, 1995, **66**, 63–68.
- U. Rychlewska, M. B. H. Broom, D. S. Eggleston and D. J. Hodgson, *J. Am. Chem. Soc.*, 1985, **107**, 4768–4772.
- Y. Lu, M. Zheng, B. Wang, L. Fu, W. Zhao, P. Li, J. Xu, H. Zhu, H. Jin, D. Yin, H. Huang, A. M. Upton and Z. Ma, *Antimicrob. Agents Chemother.*, 2011, **55**, 5185–5193.
- G. Bolla and A. Nangia, *Cryst. Growth Des.*, 2012, **12**, 6250–6259.
- K. Peters, S. Leitzke, J. E. Diederichs, K. Borner, H. Hahn, R. H. Muller and S. Ehlers, *J. Antimicrob. Chemother.*, 2000, **45**, 77–83.
- T. R. Krishnan and I. Abraham, *Drug Dev. Ind. Pharm.*, 1991, **17**, 1823–1842.
- J. R. O'Reilly, O. I. Corrigan and C. M. O'Driscoll, *Int. J. Pharm.*, 1994, **109**, 147–154.
- J. R. O'Reilly, O. I. Corrigan and C. M. O'Driscoll, *Int. J. Pharm.*, 1994, **105**, 137–146.
- A. S. Narang and A. K. Srivastava, *Drug Dev. Ind. Pharm.*, 2002, **28**, 1001–1013.
- I. Hernandez-Valdepena, M. Domurado, J. Coudane, C. Braud, J. F. Baussard, M. Vert and D. Domurado, *Eur. J. Pharm. Sci.*, 2009, **36**, 345–351.
- V. Darcos, S. El Habnoui, B. Nottelet, A. El Ghzaoui and J. Coudane, *Polym. Chem.*, 2010, **1**, 280–282.
- N. Bailly, M. Thomas and B. Klumperman, *Biomacromolecules*, 2012, **13**, 4109–4117.
- M. A. Schott, M. Domurado, L. Leclercq, C. Barbaud and D. Domurado, *Biomacromolecules*, 2013, **14**, 1936–1944.
- Y. Meng, C. Wu, J. Zhang, Q. Cao, Q. Liu and Y. Yu, *Colloid J.*, 2015, **77**, 754–760.
- R. T. Mehta, *Antimicrob. Agents Chemother.*, 1996, **40**, 1893–1902.
- V. B. Patel and A. N. Misra, *J. Microencapsulation*, 1999, **16**, 357–367.
- I. Salem, *Int. J. Pharm.*, 2003, **260**, 105–114.
- P. Schwinte, M. Ramphul, R. Darcy and J. F. O'Sullivan, *J. Inclusion Phenom. Macrocyclic Chem.*, 2003, **47**, 109–112.
- I. Ghosh and W. M. Nau, *Adv. Drug Delivery Rev.*, 2012, **64**, 764–783.





32 B. Brady, R. Darcy and J. F. O'Sullivan, *J. Inclusion Phenom. Macrocyclic Chem.*, 1999, **33**, 39–46.

33 E. Masson, X. Ling, R. Joseph, L. Kyeremeh-Mensah and X. Lu, *RSC Adv.*, 2012, **2**, 1213–1247.

34 D. Shetty, J. K. Khedkar, K. M. Park and K. Kim, *Chem. Soc. Rev.*, 2015, **44**, 8747–8761.

35 S. J. Barrow, S. Kasera, M. J. Rowland, J. Del Barrio and O. A. Scherman, *Chem. Rev.*, 2015, **115**, 12320–12406.

36 K. I. Assaf and W. M. Nau, *Chem. Soc. Rev.*, 2015, **44**, 394–418.

37 J. Lagona, P. Mukhopadhyay, S. Chakrabarti and L. Isaacs, *Angew. Chem., Int. Ed.*, 2005, **44**, 4844–4870.

38 G. Hettiarachchi, D. Nguyen, J. Wu, D. Lucas, D. Ma, L. Isaacs and V. Briken, *PLoS One*, 2010, **5**, e10514.

39 V. D. Uzunova, C. Cullinane, K. Brix, W. M. Nau and A. I. Day, *Org. Biomol. Chem.*, 2010, **8**, 2037–2042.

40 H. Chen, J. Y. W. Chan, X. Yang, I. W. Wyman, D. Bardelang, D. H. Macartney, S. M. Y. Lee and R. Wang, *RSC Adv.*, 2015, **5**, 30067–30074.

41 D. H. Macartney, *Isr. J. Chem.*, 2011, **51**, 600–615.

42 R. Wang and D. H. Macartney, *Org. Biomol. Chem.*, 2008, **6**, 1955–1960.

43 R. Wang, I. W. Wyman, S. Wang and D. H. Macartney, *J. Inclusion Phenom. Macrocyclic Chem.*, 2009, **64**, 233–237.

44 S. Li, H. Yin, G. Martinz, I. W. Wyman, D. Bardelang, D. H. Macartney and R. Wang, *New J. Chem.*, 2016, **40**, 3484–3490.

45 R. Wang, L. Yuan and D. H. Macartney, *Chem. Commun.*, 2006, 2908–2910.

46 S. Li, X. Miao, I. W. Wyman, Y. Li, Y. Zheng, Y. Wang, D. H. Macartney and R. Wang, *RSC Adv.*, 2015, **5**, 56110–56115.

47 R. Wang, L. Yuan and D. H. Macartney, *Organometallics*, 2006, **25**, 1820–1823.

48 R. Wang and D. H. Macartney, *Tetrahedron Lett.*, 2008, **49**, 311–314.

49 R. Wang, B. C. Macgillivray and D. H. Macartney, *Dalton Trans.*, 2009, 3584–3589.

50 N. J. Wheate, A. I. Day, R. J. Blanch, A. P. Arnold, C. Cullinane and J. G. Collins, *Chem. Commun.*, 2004, 1424–1425.

51 Y. J. Jeon, S. Y. Kim, Y. H. Ko, S. Sakamoto, K. Yamaguchi and K. Kim, *Org. Biomol. Chem.*, 2005, **3**, 2122–2125.

52 D. Ma, B. Zhang, U. Hoffmann, M. G. Sundrup, M. Eikermann and L. Isaacs, *Angew. Chem., Int. Ed. Engl.*, 2012, **51**, 11358–11362.

53 D. H. Macartney, *Future Med. Chem.*, 2013, **5**, 2075–2089.

54 H. H. Lee, T. S. Choi, S. J. Lee, J. W. Lee, J. Park, Y. H. Ko, W. J. Kim, K. Kim and H. I. Kim, *Angew. Chem., Int. Ed. Engl.*, 2014, **53**, 7461–7465.

55 H. Chen, J. Y. W. Chan, S. Li, J. J. Liu, I. W. Wyman, S. M. Y. Lee, D. H. Macartney and R. Wang, *RSC Adv.*, 2015, **5**, 63745–63752.

56 S. Li, H. Chen, X. Yang, D. Bardelang, I. W. Wyman, J. Wan, S. M. Lee and R. Wang, *ACS Med. Chem. Lett.*, 2015, **6**, 1174–1178.

57 X. Miao, Y. Li, I. Wyman, S. M. Y. Lee, D. H. Macartney, Y. Zheng and R. Wang, *Med. Chem. Commun.*, 2015, **6**, 1370–1374.

58 A. Day, A. P. Arnold, R. J. Blanch and B. Snushall, *J. Org. Chem.*, 2001, **66**, 8094–8100.

59 M. Kurabachew, S. H. Lu, P. Krastel, E. K. Schmitt, B. L. Suresh, A. Goh, J. E. Knox, N. L. Ma, J. Jiricek, D. Beer, M. Cynamon, F. Petersen, V. Dartois, T. Keller, T. Dick and V. K. Sambandamurthy, *J. Antimicrob. Chemother.*, 2008, **62**, 713–719.

60 J. M. Quigley, K. M. S. Fahelelbom, R. F. Timoney and O. I. Corrigan, *Int. J. Pharm.*, 1990, **58**, 107–113.

61 Z. Miskolczy, M. Megyesi, G. Tarkanyi, R. Mizsei and L. Biczok, *Org. Biomol. Chem.*, 2011, **9**, 1061–1070.

62 V. Kolman, M. S. A. Khan, M. Babinsky, R. Marek and V. Sindelar, *Org. Lett.*, 2011, **13**, 6148–6151.

63 E. L. Robinson, P. Y. Zavalij and L. Isaacs, *Supramol. Chem.*, 2015, **27**, 288–297.

64 T. Higuchi and K. A. Connors, *Adv. Anal. Chem. Instrum.*, 1965, **4**, 117–212.

65 C. A. MacRae and R. T. Peterson, *Nat. Rev. Drug Discovery*, 2015, **14**, 721–731.

66 L. Xia, L. Zheng and J. L. Zhou, *J. Appl. Toxicol.*, 2016, **36**, 853–862.

67 S. Sasagawa, Y. Nishimura, J. Koiwa, T. Nomoto, T. Shintou, S. Murakami, M. Yuge, K. Kawaguchi, R. Kawase, T. Miyazaki and T. Tanaka, *ACS Chem. Biol.*, 2016, **11**, 381–388.

68 J.-t. Chen, H.-q. Sun, W.-l. Wang, W.-m. Xu, Q. He, S. Shen, J. Qian and H.-l. Gao, *Acta Pharmacol. Sin.*, 2015, **36**, 1349–1355.